



**HAL**  
open science

## Controlling the nanomorphology of thin conformal Cu<sub>2</sub>S overlayers grown on Cu<sub>2</sub>O compact layers and nanowires

Ignacio Mínguez-Bacho, Marc Courté, Chen Shi, Denis Fichou

► **To cite this version:**

Ignacio Mínguez-Bacho, Marc Courté, Chen Shi, Denis Fichou. Controlling the nanomorphology of thin conformal Cu<sub>2</sub>S overlayers grown on Cu<sub>2</sub>O compact layers and nanowires. *Materials Letters*, 2015, 159, pp.47-50. 10.1016/j.matlet.2015.06.064 . hal-01172703

**HAL Id: hal-01172703**

**<https://hal.sorbonne-universite.fr/hal-01172703>**

Submitted on 7 Jul 2015

**HAL** is a multi-disciplinary open access archive for the deposit and dissemination of scientific research documents, whether they are published or not. The documents may come from teaching and research institutions in France or abroad, or from public or private research centers.

L'archive ouverte pluridisciplinaire **HAL**, est destinée au dépôt et à la diffusion de documents scientifiques de niveau recherche, publiés ou non, émanant des établissements d'enseignement et de recherche français ou étrangers, des laboratoires publics ou privés.

# Controlling the nanomorphology of thin conformal Cu<sub>2</sub>S overlayers grown on Cu<sub>2</sub>O compact layers and nanowires

Ignacio Mínguez-Bacho,<sup>a</sup> Marc Courté,<sup>a</sup> Chen Shi,<sup>a</sup> and Denis Fichou\*<sup>a,b,c</sup>

<sup>a</sup> School of Physical and Mathematical Sciences, Nanyang Technological University, 637371, Singapore.

<sup>b</sup> Sorbonne Universités, UPMC Univ Paris 06, UMR 8232, Institut Parisien de Chimie Moléculaire, F-75005, Paris, France. Tel: +33144275080; E-mail: denis.fichou@upmc.fr

<sup>c</sup> CNRS, UMR 8232, Institut Parisien de Chimie Moléculaire, F-75005, Paris, France

## Abstract

Thin conformal Cu<sub>2</sub>S overlayers are grown on Cu<sub>2</sub>O compact layers (CLs) and nanowires (NWs) by ion exchange reaction (IER). This method is based on the exchange of O<sup>2-</sup> into S<sup>2-</sup> ions at the surface of Cu<sub>2</sub>O in a solution-containing Na<sub>2</sub>S acting as the sulphur ions source. The Cu<sub>2</sub>S overlayers are grown under different experimental conditions by varying the Na<sub>2</sub>S concentration and the duration of the IER process, thus leading to different Cu<sub>2</sub>S nanomorphologies. In particular, when a concentration of 2 mM Na<sub>2</sub>S is used, hexagonal Cu<sub>2</sub>S nanocrystals are formed on the surface of both Cu<sub>2</sub>O CLs and NWs. These nanocrystals are of larger size at the ridges of the Cu<sub>2</sub>O cubes in CLs and at the tips of Cu<sub>2</sub>O in NWs. The high-quality crystal structure and composition of Cu<sub>2</sub>S are confirmed by high resolution transmission electron spectroscopy and X-ray photoluminescence spectroscopy.

**Keywords:** Ion exchange reaction; nanomorphology; overlayer; copper oxide; copper sulfide.

## 1. Introduction

Nanostructured metal chalcogenides are attracting considerable attention due to their exceptional physical and chemical properties [1, 2]. Applications of these materials are as diverse as thermoelectrical systems, memories, energy conversion, and energy storage devices [3]. Cu<sub>2</sub>S is a typical metal chalcogenide behaves as a p-type semiconductor with an indirect band gap  $E_g=1.2$  eV. Depending on the preparation method, Cu<sub>2</sub>S thin films can adopt variety morphologies such as nanowires [4], nanocages [5] or nanoparticles with different geometries [6]. Nanostructured Cu<sub>2</sub>S is

used in lithium ion batteries [7], quantum dots solar cells as counter-electrodes [8] or photovoltaic devices [9].  $\text{Cu}_2\text{S}$  can be prepared by atomic layer deposition [10], physical vapor deposition [11] or hydrothermal [12], among others.

Together with several other metal oxides [13-15] cuprous oxide  $\text{Cu}_2\text{O}$  is a promising material for photoelectrochemical (PEC) solar energy conversion [16]. In this work we report the preparation and nanomorphology of thin conformal  $\text{Cu}_2\text{S}$  overlayers grown on  $\text{Cu}_2\text{O}$  compact layers (CLs) and nanowires (NWs). The  $\text{Cu}_2\text{S}$  overlayers are grown via an ion exchange reaction (IER) consisting in the exchange of oxygen ions from  $\text{Cu}_2\text{O}$  with sulfur ions from  $\text{Na}_2\text{S}$  contained in an aqueous solution. The nanomorphology of the  $\text{Cu}_2\text{S}$  overlayers can be precisely controlled by adjusting the  $\text{Na}_2\text{S}$  concentration and the IER reaction time, and is independent of the starting  $\text{Cu}_2\text{O}$  morphology, either CLs or NWs.

## 2. Materials and methods

$\text{Cu}_2\text{O}$  nanostructures are fabricated as CLs by electrodeposition (see Electronic Supplementary Material ESM†, Section 1.1) and as NWs by anodization (ESM† Section 1.2). Then  $\text{Cu}_2\text{O}$  CLs and NWs (Fig. S1) are used for growing  $\text{Cu}_2\text{S}$  overlayers by IER. Different  $\text{Cu}_2\text{O}$  samples are immersed in 2 mM and 5 mM  $\text{Na}_2\text{S}$  solutions during different times at 80 °C (ESM†, Section 1.3). All materials are analyzed by scanning electron microscopy (SEM, Jeol JSM-6700F) and high-resolution transmission electron microscopy (HR-TEM, JEM-2010). The HR-TEM analysis is carried out on the samples in powder form. Absolute ethanol is added to the powder in a 10 ml bottle and deposited three drops at intervals of 5 minutes on copper grids. X-ray photoelectron spectroscopy (XPS) was performed under monochromatic Al  $K\alpha$  radiation ( $h\nu=1486.7$  eV) was used at 300 W, 14 kV under ultra-high vacuum.

## 3. Results and discussion

### 3.1 Morphology of the $\text{Cu}_2\text{S}$ overlayers

When carried out during 15 minutes in a 2 mM solution, the IER growth of  $\text{Cu}_2\text{S}$  is slow (Fig 1a,b). It induces the formation of a homogeneous layer of nanostructured  $\text{Cu}_2\text{S}$  crystals all over the surface of the  $\text{Cu}_2\text{O}$  CLs (Fig. 1a). The  $\text{Cu}_2\text{S}$  nanocrystals grow preferentially on the ridges of the cubic  $\text{Cu}_2\text{O}$  structures (Fig. 1b,c). These crystals are of larger size than those growing on the faces of the  $\text{Cu}_2\text{O}$  cubes (Fig. 1d). As expected the  $\text{Cu}_2\text{S}$  nanocrystals are hexagonal in shape. A longer IER duration time up to 60 minutes does not affect drastically the morphology of the  $\text{Cu}_2\text{S}$  overlayer (Fig. 1e), although a thickening of the  $\text{Cu}_2\text{S}$  crystals on the ridges progressively takes place due to an

increasing overlap of the crystals (Fig. 1f). Besides, when the  $\text{Na}_2\text{S}$  concentration is increased up to 5 mM, the  $\text{Cu}_2\text{S}$  growth kinetics is faster and takes place in only 2 minutes (Fig. 1g). The  $\text{Cu}_2\text{S}$  overlayer is also very homogeneous, although there are no nanostructures formed on the surface (Fig. 1h,i). A perpendicular cross-arrangement of the constitutive  $\text{Cu}_2\text{S}$  nanocrystals is clearly observed that is similar to that observed in a 2 mM  $\text{Na}_2\text{S}$  solution after 15 minutes (Fig. 1d). Finally, when  $\text{Cu}_2\text{O}$  is immersed in a 2 mM solution, adhesion of the  $\text{Cu}_2\text{S}$  overlayer on  $\text{Cu}_2\text{O}$  CLs is excellent, thus making potential applications realistic. However, we note that adhesion of the  $\text{Cu}_2\text{S}$  overlayer is reduced when using a higher  $\text{Na}_2\text{S}$  concentration of 5 mM, thus leading to partial detachment of the  $\text{Cu}_2\text{S}$  overlayer.

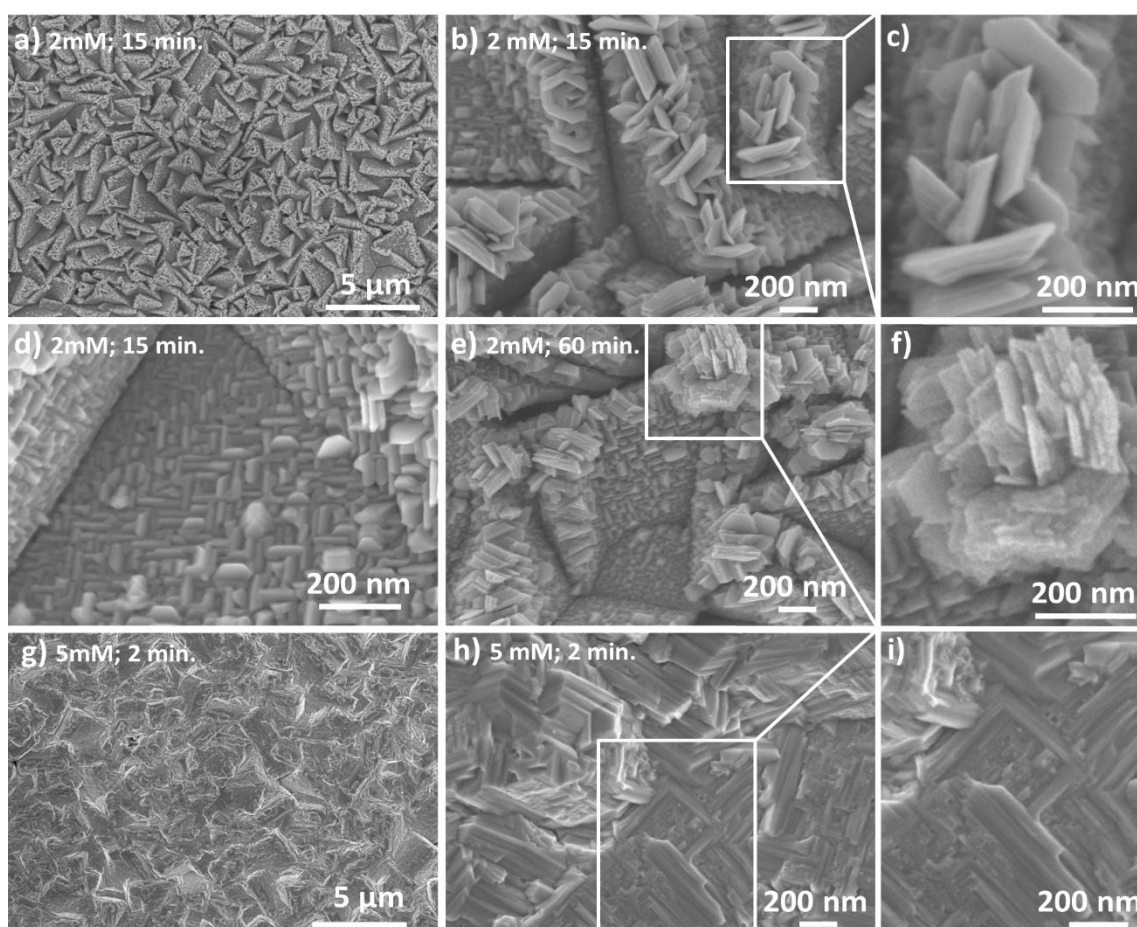


**Fig. 1** SEM micrographs of  $\text{Cu}_2\text{O}$  compact layers (CLs) coated with a  $\text{Cu}_2\text{S}$  overlayer prepared by IER under different  $\text{Na}_2\text{S}$  concentrations and reaction times. Magnifications of the  $\text{Cu}_2\text{S}$  nanocrystals inside the white squares are shown on the right images.

IER has been also conducted on  $\text{Cu}_2\text{O}$  NWs in solutions containing  $\text{Na}_2\text{S}$  concentrations of respectively 2 mM and 5 mM. After 30 minutes of IER in a 2 mM solution an overlayer of  $\text{Cu}_2\text{S}$  nanocrystals grows around the NWs (Fig. 2a). The morphology of the  $\text{Cu}_2\text{S}$  layer (Fig. 2b) is comparable to that obtained in similar conditions on CLs (Fig. 1b,e). Noticeably, larger  $\text{Cu}_2\text{S}$

nanostructures grow on the  $\text{Cu}_2\text{O}$  NWs tips, a phenomenon which is reminiscent of the higher concentration of  $\text{Cu}_2\text{S}$  nanocrystals on the  $\text{Cu}_2\text{O}$  CLs ridges (*vide supra*). On the other hand, when the IER process is carried out in a 5 mM solution, the  $\text{Cu}_2\text{S}$  overlayer is not nanostructured (Fig. 2c) although the  $\text{Cu}_2\text{S}$  crystal structure formed after 5 minutes is still visible (Fig. 2d). This morphology resembles that of the  $\text{Cu}_2\text{S}$ -coated  $\text{Cu}_2\text{O}$  CLs grown into a 5 mM solution (see Fig. 1h,i). However, in contrast to  $\text{Cu}_2\text{S}$  overlayers grown on CLs using a 5 mM  $\text{Na}_2\text{S}$  concentration, the  $\text{Cu}_2\text{S}$  overlayers grown on NWs in 5 mM solutions exhibit a very good adhesion to  $\text{Cu}_2\text{O}$ .

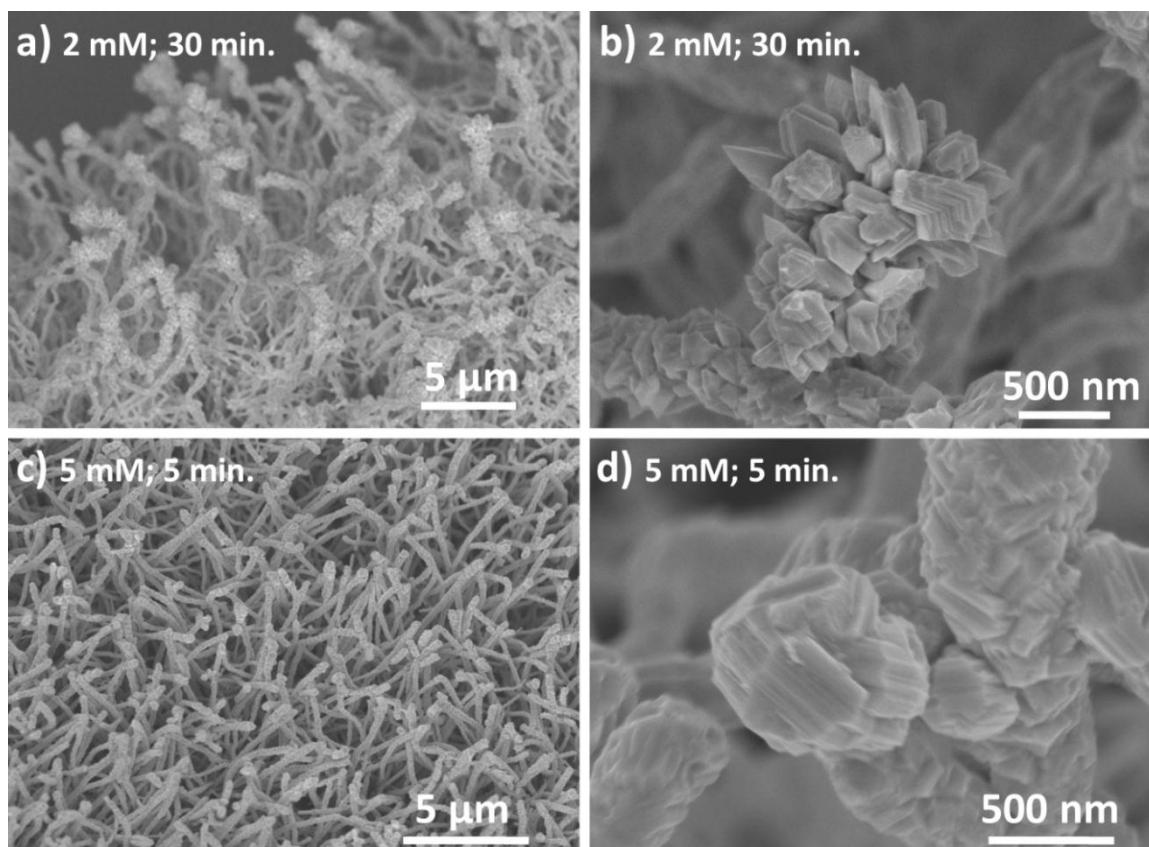


**Fig. 2** SEM micrographs of  $\text{Cu}_2\text{O}$  nanowires (NWs) coated by a  $\text{Cu}_2\text{S}$  overlayer prepared an IER process under different  $\text{Na}_2\text{S}$  concentrations and reaction times.

### 3.2 High resolution transmission electron microscopy (HR-TEM)

Images in Fig. 3a,b correspond to  $\text{Cu}_2\text{S}$ -coated  $\text{Cu}_2\text{O}$  samples for respectively a CLs and NWs. In both images dark and bright areas are observed. The selected regions delimited by white squares are analysed by fast Fourier transform (FFT). Fig. 3c represents the FFT performed in the selected region of the brighter area of a CL. It reveals lattice spacing of 3.19, 2.78 and 1.96 Å which can be attributed to the (111), (200) and (220) planes of  $\text{Cu}_2\text{S}$ . In the FFT of the selected region in darker area (Fig. 3d), three lattice spacing of 2.45, 2.13 and 1.50 Å are observed that can be attributed respectively to the crystallographic planes (111), (200) and (220) of  $\text{Cu}_2\text{O}$ . The FFT analysis of the bright selected area of

the NWs (Fig. 3e) reveals an interplanar distance of 1.96 Å corresponding to the (220) plane of  $\text{Cu}_2\text{S}$ . It also unveils the (200) plane corresponding to  $\text{Cu}_2\text{O}$  with a interplanar distance of 2.13 Å. The crystallographic planes of  $\text{Cu}_2\text{O}$  are also observed very clearly in the FFT of the region in the darker area (Fig. 3f).

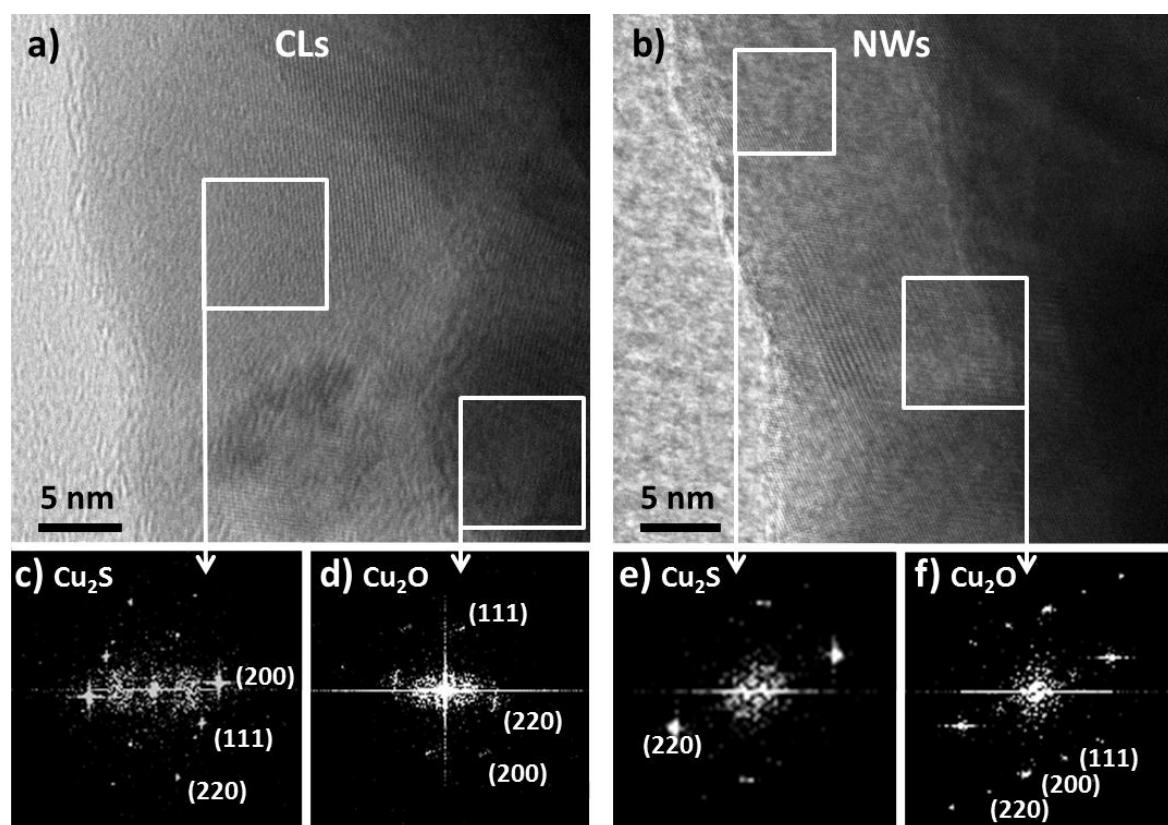


**Fig. 3** HR-TEM images of  $\text{Cu}_2\text{S}$ -coated  $\text{Cu}_2\text{O}$  a) CLs and b) NWs. c,d,e,f) FFT analysis of the selected regions in either dark or bright contrast (white squares)

### 3.3 X-ray photoluminescence spectroscopy (XPS)

We performed X-ray photoelectron spectroscopy (XPS) in order to confirm the formation of  $\text{Cu}_2\text{S}$  (Fig. 4). In the wide XPS spectra are shown the Cu 2p, Cu LMM, O 1s, C 1s and S 2p for both CLs and NWs (Fig. 4a,b). We can observe the Cu 2p<sub>1/2</sub> peak at 952.5 eV and the Cu 2p<sub>3/2</sub> peak at 932.6 eV (Fig. 4c) showing that the oxidation state of copper species correspond to  $\text{Cu}^+$ . We have seen no satellite peaks of Cu 2p<sub>1/2</sub> and Cu 2p<sub>3/2</sub> which is an evidence of the absence of  $\text{Cu}^{2+}$  oxidation state on the surface of the overlayers on CLs and NWs. For both CLs and NWs the S 2p regions (Fig. 4d) show the characteristic shape of an  $\text{S}^{2-}$  band. Peaks at 162.9 eV and 161.8 eV can be attributed to the S 2p<sub>1/2</sub> and S 2p<sub>3/2</sub> spin-orbit doublet.

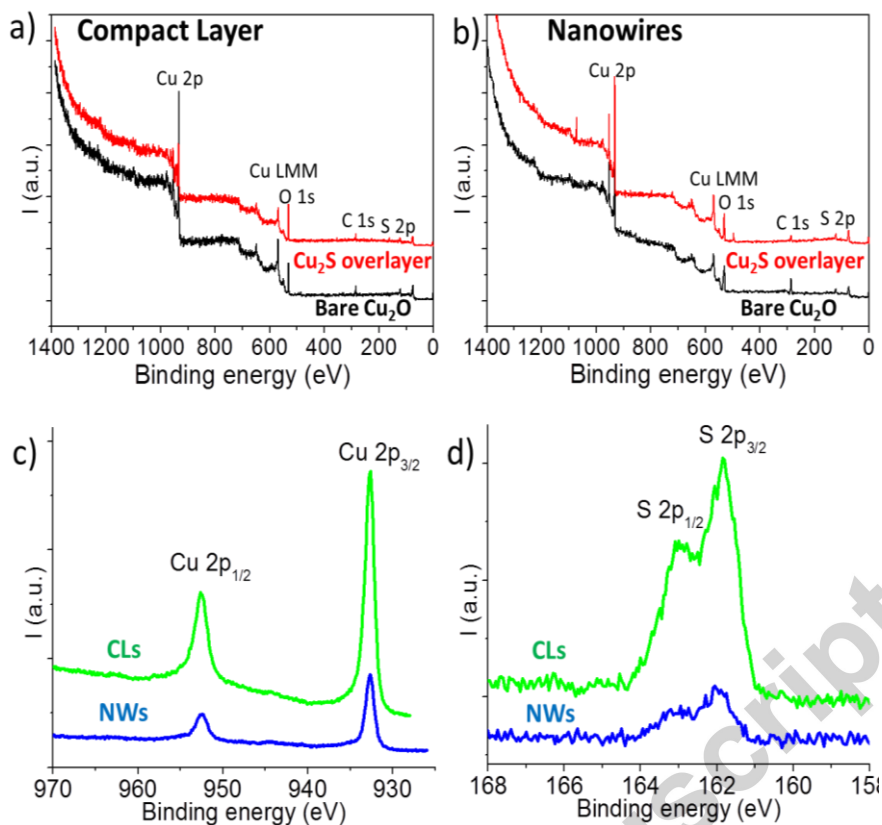


**Fig. 4** a,b) Wide scan XPS spectra of  $\text{Cu}_2\text{O}$  CLs and NWs with (red) and without (black)  $\text{Cu}_2\text{S}$  overlayers. c,d) XPS spectra of the  $\text{Cu}2p$  and  $\text{S}2p$  regions of the  $\text{Cu}_2\text{S}$  overlayers on CLs (green) and NWs (blue).

#### 4. Conclusion

The influence of the concentration of  $\text{Na}_2\text{S}$  solution is a critical parameter for the growth of the  $\text{Cu}_2\text{S}$  overlayers on  $\text{Cu}_2\text{O}$  compact layers and nanowires by ion exchange reaction. When a concentration of 2 mM  $\text{Na}_2\text{S}$  is used, hexagonal  $\text{Cu}_2\text{S}$  nanocrystals are formed on the surface of both  $\text{Cu}_2\text{O}$  CLs and NWs. The sizes of the crystals are bigger at the ridges of the  $\text{Cu}_2\text{O}$  cubes in CLs and the tips of  $\text{Cu}_2\text{O}$  in NWs. The time scale of the IER process does not affect much the  $\text{Cu}_2\text{S}$  morphology although larger clusters of  $\text{Cu}_2\text{S}$  nanocrystals are formed at the ridges of the CLs. HR-TEM confirms the formation of the  $\text{Cu}_2\text{S}$  single crystals while XPS reveals the high-quality chemical composition of the overlayers. We are presently using these conformal  $\text{Cu}_2\text{S}$  overlayers to protect  $\text{Cu}_2\text{O}$  electrodes during photoelectrochemical experiments that will be reported elsewhere [17].

#### Acknowledgements

The authors wish to thank the support from the Ministry of Education in Singapore under the AcRF Tier 2 (MOE2014-T2-1-132). The authors kindly acknowledge Prof. H. J. Fan (SPMS/NTU) for fruitful discussions and Z. Fan (SPMS/NTU) for his contribution in HR-TEM experiments.

## References

- [1] Gao M-R, Jiang J, Yu S-H. Solution-Based Synthesis and Design of Late Transition Metal Chalcogenide Materials for Oxygen Reduction Reaction. *Small* 2012;8:13-27.
- [2] Osterloh FE. Inorganic nanostructures for photoelectrochemical and photocatalytic water splitting. *Chem Soc Rev* 2013;42:2294-320.
- [3] Gao M-R, Xu Y-F, Jiang J, Yu S-H. Nanostructured metal chalcogenides: synthesis, modification, and applications in energy conversion and storage devices. *Chem Soc Rev* 2013;42:2986-3017.
- [4] Liu ZP, Xu D, Liang JB, Shen JM, Zhang SY, Qian YT. Growth of Cu<sub>2</sub>S ultrathin nanowires in a binary surfactant solvent. *J Phys Chem B* 2005;109:10699-704.
- [5] Kuo CH, Chu YT, Song YF, Huang MH. Cu<sub>2</sub>O Nanocrystal-Templated Growth of Cu<sub>2</sub>S Nanocages with Encapsulated Au Nanoparticles and In-Situ Transmission X-ray Microscopy Study. *Adv Funct Mater* 2011;21:792-7.
- [6] Li W, Shavel A, Guzman R, Rubio-Garcia J, Flox C, Fan JD, Cadavid D, Ibanez M, Arbiol J, Morante JR, Cabot A. Morphology evolution of Cu<sub>2-x</sub>S nanoparticles: from spheres to dodecahedrons. *Chem Commun* 2011;47:10332-4.
- [7] Lai CH, Huang KW, Cheng JH, Lee CY, Hwang BJ, Chen LJ. Direct growth of high-rate capability and high capacity copper sulfide nanowire array cathodes for lithium-ion batteries. *J Mater Chem* 2010;20:6638-45.
- [8] Peng Z, Liu Y, Zhao Y, Chen K, Cheng Y, Chen W. Incorporation of the TiO<sub>2</sub> nanowire arrays photoanode and Cu<sub>2</sub>S nanorod arrays counter electrode on the photovoltaic performance of quantum dot sensitized solar cells. *Electrochim Acta* 2014;135:276-83.
- [9] Riha SC, Jin S, Baryshev SV, Thimsen E, Wiederrecht GP, Martinson ABF. Stabilizing Cu<sub>2</sub>S for Photovoltaics One Atomic Layer at a Time. *ACS Appl Mater Interf* 2013;5:10302-9.
- [10] Martinson ABF, Riha SC, Thimsen E, Elam JW, Pellin MJ. Structural, optical, and electronic stability of copper sulfide thin films grown by atomic layer deposition. *Energ Environ Sci* 2013;6:1868-78.
- [11] Siol S, Sträter H, Brüggemann R, Brötz J, Bauer GH, Klein A, et al. PVD of copper sulfide (Cu<sub>2</sub>S) for PIN-structured solar cells. *J Phys D Appl Phys* 2013;46:495112.
- [12] Yu X, An X. Controllable hydrothermal synthesis of Cu<sub>2</sub>S nanowires on the copper substrate. *Mater Lett* 2010;64:252-4.
- [13] Qi H, Wolfe J, Wang D, Fan HJ, Fichou D, Chen Z. Triple-layered nanostructured WO<sub>3</sub> photoanodes with enhanced photocurrent generation and superior stability for photoelectrochemical solar energy conversion. *Nanoscale* 2014;6:13457-62.



- [14] Fichou D, Pouliquen J, Kossanyi J, Jakani M, Campet G, Claverie J. Extension of the photoresponse of semiconducting zinc-oxide electrodes by 3d impurities absorbing in the visible region of the solar spectrum. *J Electroanal Chem* 1985;188:167-87.
- [15] Jakani M, Campet G, Claverie J, Fichou D, Pouliquen J, Kossanyi J. Photoelectrochemical properties of zinc oxide doped with 3d elements. *J Solid State Chem* 1985;56:269-77
- [16] Paracchino A, Mathews N, Hisatomi T, Stefiak M, Tilley SD, Grätzel M. Ultrathin films on copper(I) oxide water splitting photocathodes: a study on performance and stability. *Energ Environ Sci* 2012;5:8673-81.
- [17] Minguez-Bacho I, Courté M, Fan HJ and Fichou D. Conformal Cu<sub>2</sub>S-coated Cu<sub>2</sub>O nanostructures grown by ion exchange reaction and their photoelectrochemical properties *Nanotechnology* 2015;26:185401.

### Highlights

- Conformal layers of Cu<sub>2</sub>S on Cu<sub>2</sub>O are grown by ion exchange reaction.
- The morphology of the Cu<sub>2</sub>S overlayers is not dictated by the morphology of the starting Cu<sub>2</sub>O material.
- Different Cu<sub>2</sub>S nanomorphologies are studied by SEM, HRTEM and XPS.
- Cu<sub>2</sub>S overlayers have a potential application as protection against photodecomposition of Cu<sub>2</sub>O photoelectrodes.